# Scalable and Highly Porous Membrane Adsorbents for Direct Air Capture of CO<sub>2</sub>

Thien Tran<sup>a,b,c</sup>, Shweta Singh<sup>a</sup>, Shiwang Cheng<sup>d</sup>, and Haiqing Lin<sup>a,\*</sup>

<sup>a</sup> Department of Chemical and Biological Engineering, University at Buffalo, The State

University of New York, Buffalo, NY 14260, USA

<sup>b</sup> U.S. Department of Energy, National Energy Technology Laboratory, Pittsburgh, PA

15236, USA

<sup>c</sup> NETL Support Contractor, Pittsburgh, PA 15236, USA

<sup>d</sup> Department of Chemical Engineering and Materials Science, Michigan State University,

East Lansing, MI 48824, USA

\*Corresponding author: <a href="mailto:haiqingl@buffalo.edu">haiqingl@buffalo.edu</a> (H.Lin)

**KEYWORDS:** *direct air capture, polyethylenimine, membrane adsorbent, CO<sub>2</sub> sorption,* 

porous support

ABSTRACT: Direct air capture (DAC) of CO<sub>2</sub> is a carbon-negative technology to mitigate carbon emissions, and it requires low-cost sorbents with high CO<sub>2</sub> sorption capacity that can be easily manufactured on a large scale. In this work, we develop highly porous membrane adsorbents comprising branched polyethylenimine (PEI) impregnated in low-cost, porous Solupor supports. The effect of the PEI molecular mass and loading on the physical properties of the adsorbents is evaluated, including porosity, degradation temperature, glass transition temperature, and CO<sub>2</sub> permeance. CO<sub>2</sub> capture capacity from simulated air containing 400 ppm CO<sub>2</sub> in these sorbents is thoroughly investigated as a function of temperature and relative humidity (RH). Polymer dynamics was examined using differential scanning calorimetry (DSC) and broadband dielectric spectroscopy (BDS), showing that CO<sub>2</sub> sorption is limited by its diffusion in these PEI-based sorbents. A membrane adsorbent containing 48 mass% PEI (800 Da) with a porosity of 72% exhibits a CO<sub>2</sub> sorption capacity of 1.2 mmol/g at 25 °C and RH of 30%, comparable to the state-of-the-art adsorbents. Multi-cycles of sorption and desorption were performed to determine their regenerability, stability, and potential for practical applications.

## ■ INTRODUCTION

Direct air capture (DAC) has emerged as a critical approach to reducing CO<sub>2</sub> content and ultimately mitigating the long-lasting effect of CO<sub>2</sub> in the atmosphere.<sup>1, 2</sup> The main challenge to the DAC is the low CO<sub>2</sub> content (~400 ppm) in the air and thus associated high cost.<sup>3, 4</sup> For example, the CO<sub>2</sub> content in the air is 300 times more dilute than in coal-fired power plant flue gas (~12%). State-of-the-art technologies for DAC are based on solvents or sorbents, such as aqueous hydroxide solutions and solid amine sorbents.<sup>5-7</sup> The hydroxide solutions have a high capacity for CO<sub>2</sub> sorption. However, sorbent regeneration can be costly due to heating and water evaporation.<sup>8</sup>

Solid sorbents offer the possibility of low energy input, low operating costs, and good scalability. Amine groups are the key to achieving high CO<sub>2</sub> sorption capacity and high selectivity over the major components in the air (such as N<sub>2</sub> and O<sub>2</sub>). <sup>9, 10</sup> Equations 1 and 2 elucidate the reaction mechanisms between the primary and secondary amines and CO<sub>2</sub>. Under dry conditions, these amines react with CO<sub>2</sub> and form ammonium carbamate. <sup>7,11</sup> The maximum molar ratio of CO<sub>2</sub>/N can be as high as 0.5 and can increase to 1.0 in the presence of moisture, as shown in Equation 3. Equation 4 also shows that tertiary amines can react with CO<sub>2</sub> at a 1:1 molar ratio in the presence of water vapor:

$$CO_2 + 2RNH_2 \leftrightarrow RNH_3^+ + RNHCOO^- \tag{1}$$

$$CO_2 + 2R_1R_2NH \leftrightarrow R_1R_2NH_2^+ + R_1R_2NCOO^-$$
 (2)

$$CO_2 + R_1 R_2 NH + H_2 O \leftrightarrow R_1 R_2 NH_2^+ HCO_3^-$$
 (3)

$$CO_2 + R_1 R_2 R_3 N + H_2 O \leftrightarrow R_1 R_2 R_3 N H^+ H C O_3^-$$
 (4)

Amine groups can be incorporated into solid sorbents by impregnation in porous supports.<sup>6,7,12</sup> A variety of inorganic porous supports have been explored to incorporate amines including fume silica,<sup>13</sup> silica monoliths,<sup>14</sup> ordered mesoporous silica such as MCM-41 with regular cylindrical mesopores<sup>15</sup> and SBA-15 with both mesopores and intrawall pores,<sup>16</sup>

mesoporous γ alumina, <sup>17</sup> and metal-organic frameworks (MOFs). <sup>18-20</sup> CO<sub>2</sub> sorption capacity as high as 1 – 3 mmol/g was reported for simulated air. The sorption is often subject to slow kinetics due to CO<sub>2</sub> diffusion, and the pore structure and chemistry exert significant influence on CO<sub>2</sub> sorption capacity and kinetics. <sup>21, 22</sup> The strong interactions between amines and CO<sub>2</sub> may also retard CO<sub>2</sub> diffusion at low temperatures. <sup>23, 24</sup> For example, CO<sub>2</sub> sorption in a polyethylenimine (PEI)-modified silica is higher at 75 °C than 25 °C because of the faster diffusion at the higher temperature. <sup>13, 25</sup> These inorganic supports are relatively expensive to produce at a large scale. By contrast, polymeric supports (such as expanded poly(tetrafluoroethylene)<sup>26</sup> and hollow fiber membranes (HFM)<sup>27-29</sup>) have been explored as they can be low-cost and routinely produced on a large scale. Nevertheless, porous supports can be continuously optimized to lower adsorbent costs, a key component determining the DAC costs.

In this study, we develop a scalable, highly porous membrane adsorbent platform, where branched PEI is impregnated into commercial flatsheet Solupor support (20-100  $\mu$ m), as shown in Fig. 1. Solupor support is made of high-density polyethylene (HDPE), and it has a porosity of 88%, a pore size of 0.9  $\mu$ m, and good chemical and mechanical stability.<sup>30</sup> It is produced at a low cost and large scale as battery spacers, and its high porosity renders a high surface area and increases the accessibility of the amines to CO<sub>2</sub>. Two branched PEIs with molecular mass ( $M_W$ ) of 800 and 25,000 g/mol are used to elucidate their effect on CO<sub>2</sub> sorption capacity and long-term stability.<sup>31, 32</sup> The sorbents are denoted as SPEI800-x or SPEI25k-x, where x (mass%) is the PEI mass percentage in the samples. The effect of the PEI  $M_W$  and content on porosity, CO<sub>2</sub> permeance, and amine sorption efficiency is investigated. CO<sub>2</sub> sorption capacity was thoroughly evaluated as a function of temperature and relative humidity (RH) in both series of SPEIs, and their long-term stability was examined by multi-cycles of sorption and desorption. Compared with many PEI-based sorbents reported in the literature.

our highly porous adsorbents are based on commercially available low-cost supports and can be produced using existing membrane fabrication equipment and allow for similar CO<sub>2</sub> capture as packed bed systems or plate-and-frame modules while significantly reducing pressure drop and accelerating the sorption and desorption. Our membrane adsorbents demonstrate a CO<sub>2</sub> sorption capacity of 1.2 mmol/g sorbent with simulated air, comparable to state-of-the-art sorbents, making them attractive, considering their low cost and easy production scale-up. Moreover, this study, for the first time, shows that the impregnated PEI thin films have reduced chain dynamics using differential scanning calorimetry (DSC) and broadband dielectric spectroscopy (BDS), validating that the CO<sub>2</sub> sorption is limited by its diffusion in these amine-based DAC sorbents.

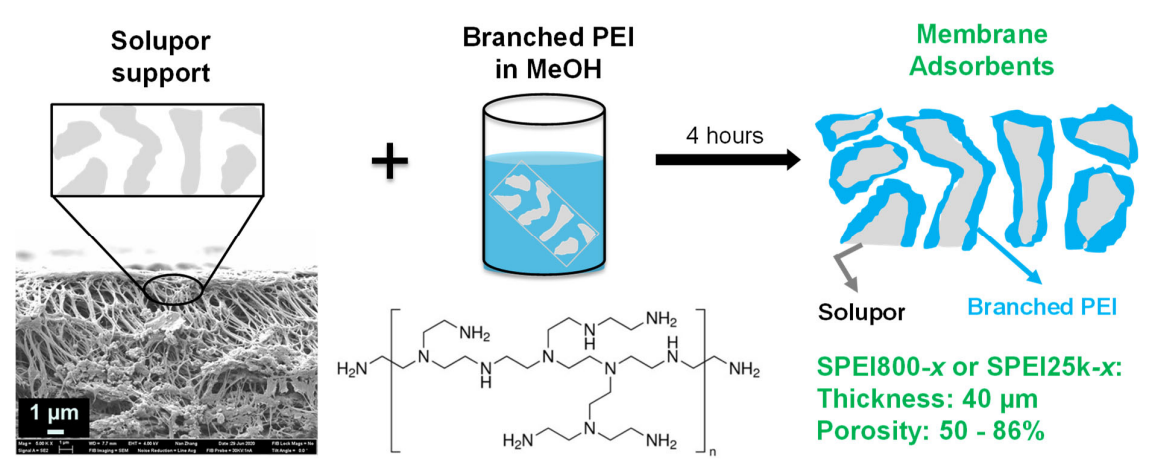


**Figure 1.** Schematic of preparation of membrane adsorbents (SPEI800-x or SPEI25k-x) via wet impregnation, including a cross-sectional SEM image of the Solupor support with a pore size ( $d_p$ ) of 0.9  $\mu$ m and a thickness of 40  $\mu$ m.

## ■ RESULTS AND DISCUSSION

**Physical Properties of Membrane Adsorbents.** The PEI loading in membrane adsorbents was determined by the mass increase after the PEI impregnation. Figure 2a shows that the PEI loading increases before leveling off with increasing PEI concentration ( $w_{PEI}$ ) in the methanol solutions. As the PEI800 concentration increases from 1 to 15 w/v% (g per 100 ml methanol), the x increases from 18% to 63% (Table S1), indicating successful loading of

PEI in the Solupor. Additionally, once the  $w_{PEI}$  is above 5 w/v%, its further increase does not significantly increase the PEI loading in the adsorbents. Assuming that the Solupor support is fully filled by the solution before drying for the PEI to coat the pore surface, the x can also be estimated using the following equation:

$$x = \frac{\phi_{SS} \times w_{PEI}}{\rho_{SS} + \phi_{SS} \times w_{PEI}} \times 100\% \tag{5}$$

where  $\phi_{SS}$  is the porosity of the Solupor support (0.88), and  $\rho_{SS}$  is the density of the Solupor support (0.13 g/cm<sup>3</sup>). As shown in Figure 2a, Equation 5 underestimates the loading for both series of adsorbents, probably because the PEI may also deposit on the Solupor surface.

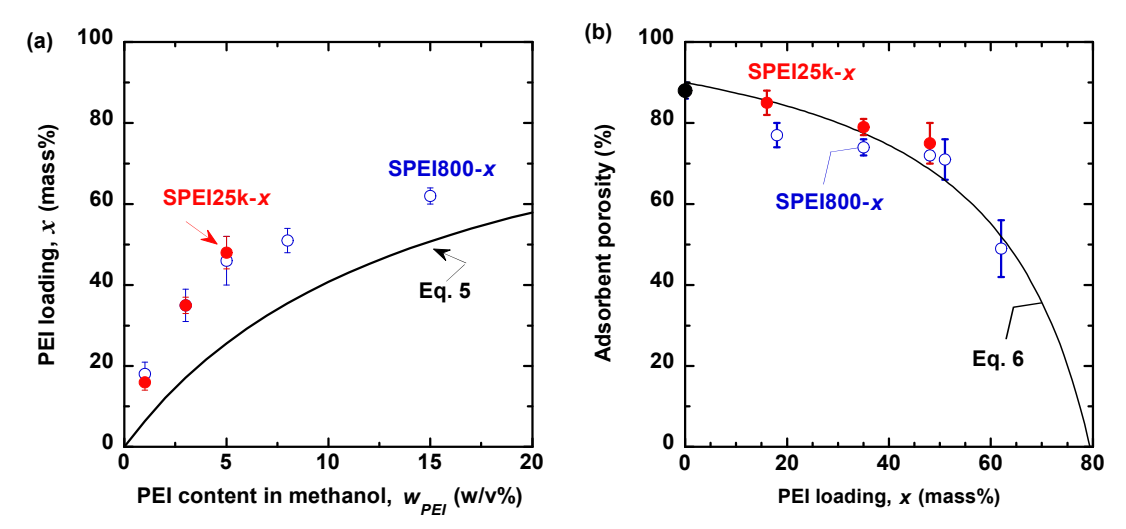


**Figure 2.** Modeling of the PEI loading (determined by the mass increase after impregnation) and porosity (determined by the solvent uptake) of the SPEIs. (a) Correlation between x and PEI concentration in the methanol solutions ( $w_{PEI}$ ). (b) Correlation between the membrane porosity and x. The error bar is the standard deviation of 3 samples or more.

The membrane porosity was determined using the n-decane sorption experiments. Figure 2b demonstrates that the membrane porosity decreases with increasing PEI loading as the pores are filled up by PEI. For example, SPEI800-18 exhibits a porosity of 76%, much higher than SPEI800-63 (49%). Similar behavior has also been observed for PEI impregnated in other supports, such as SBA-15<sup>16</sup> and MIL-101(Cr). The porosity of the membrane adsorbents ( $\phi_{MA}$ ) can also be estimated by Equation 6:

$$\phi_{MA} = \phi_{SS} - \frac{x\rho_{SS}}{(1-x)\cdot\rho_{PEI}} \tag{6}$$

As shown in Figure 2b, there is a remarkable agreement between the calculated and measured porosity.

Figures 3a and S1a display the thermograms of thermalgravimetric analysis (TGA) for Solupor, SPEI800-18, and PEI800. The Solupor support degrades at ≈490 °C, consistent with the degradation temperature of HDPE.<sup>33</sup> The pure PEI800 starts to degrade at 150 °C.<sup>34</sup> By contrast, the SPE800-18 exhibits the first degradation step from 220 to 450 °C, indicating improved thermal stability because of Solupor confinement. The mass loss of the SPEI800-18 at 450 °C is 14%, consistent with the PEI loading (18%) determined from the mass increase during the impregnation, and similar behaviors have been observed for other SPEI samples (Table S1). The second degradation step of the SPE800-18 occurs at 450 °C because of the degradation of Solupor.

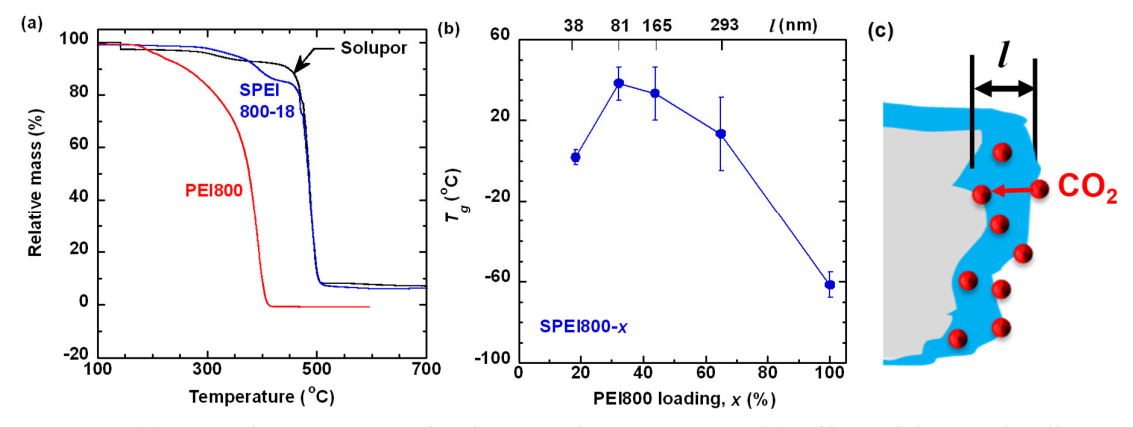


**Figure 3.** (a) TGA thermograms of Solupor and SPEI800-18. (b) Effect of the PEI loading and film thickness on  $T_g$ . (c) Schematic demonstrating CO<sub>2</sub> diffusion into PEI film. The error bar in (b) is the standard deviation for 3 samples or more.

Figure 3b shows that the glass transition temperature ( $T_g$ ) of the PEI in the SPEI800 increases with increasing loading before decreasing. For example, SPEI800-18 exhibits a  $T_g$  of 0 °C, much higher than that of PEI800 (-65 °C). The uncertainty is higher for SPEI800-49 and SPEI800-63 due to the random distribution of PEI800 in the pores at higher loadings.<sup>35</sup> To

elucidate this behavior, the average thickness of the PEI film on the pore wall, l (nm), is estimated by Equation 7:

$$l = \frac{x}{(1-x)\cdot\rho_{PEI}\cdot A_{SS}} \tag{7}$$

where  $A_{SS}$  is the surface area of the Solupor measured by the Brunauer, Emmett and Teller (BET) method (5.8 m<sup>2</sup>/g). Notably, the thickness cannot be directly measured due to the complexity of the porous structures. Therefore, the l values from Equation 7 are the only way to indicate the PEI layer thickness, which increases from 38 to 293 nm as the loading increases from 18% to 62%. Figure 3b shows that the pore wall can significantly influence the polymer chain dynamics of the thin PEI films,  $^{36, 37}$  consistent with the improved thermal stability of the Solupor-confined PEI (Figure 3a).

Table S1 also shows that increasing the x decreases pure-gas CO<sub>2</sub> permeance at 35 °C. For example, introducing 46% PEI800 in Solupor decreases CO<sub>2</sub> permeance from  $1.8 \times 10^6$  to  $2.3 \times 10^4$  GPU (1 GPU =  $10^{-6}$  cm<sup>3</sup>(STP) cm<sup>-2</sup> s<sup>-1</sup> cmHg<sup>-1</sup>). Nevertheless, the membrane adsorbents still exhibit very high gas permeance, which is needed for the air to flow through the sorbent at low pressure drops.

CO<sub>2</sub> Sorption and Behaviors of SPEIs. The CO<sub>2</sub> sorption in the SPEIs was tested with simulated dry air containing 400 ppm CO<sub>2</sub> for 4 h at 25 °C. Figure 4a shows that increasing the PEI loading increases CO<sub>2</sub> sorption capacity before leveling off for both series of samples. For example, increasing *x* from 18% to 48% increases CO<sub>2</sub> sorption capacity by 57% from 0.30 to 0.47 mmol/g for SPEI800, while SPEI25k-48 exhibits CO<sub>2</sub> sorption capacity only 25% higher than SPEI25k-16. Increasing *x* above 35% for SPEI25k and above 48 for PEI800 does not enhance CO<sub>2</sub> sorption capacity because of the limited CO<sub>2</sub> transport caused by the decreased porosity (Figure 2b) and increased PEI thickness (Figure 3b). Similar behavior has also been reported with computational simulations.<sup>15</sup>

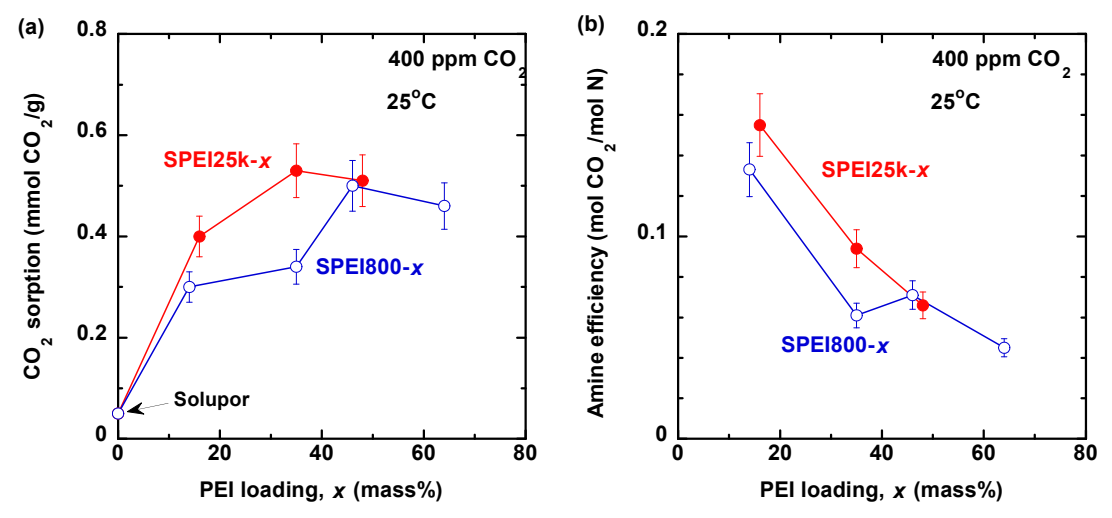
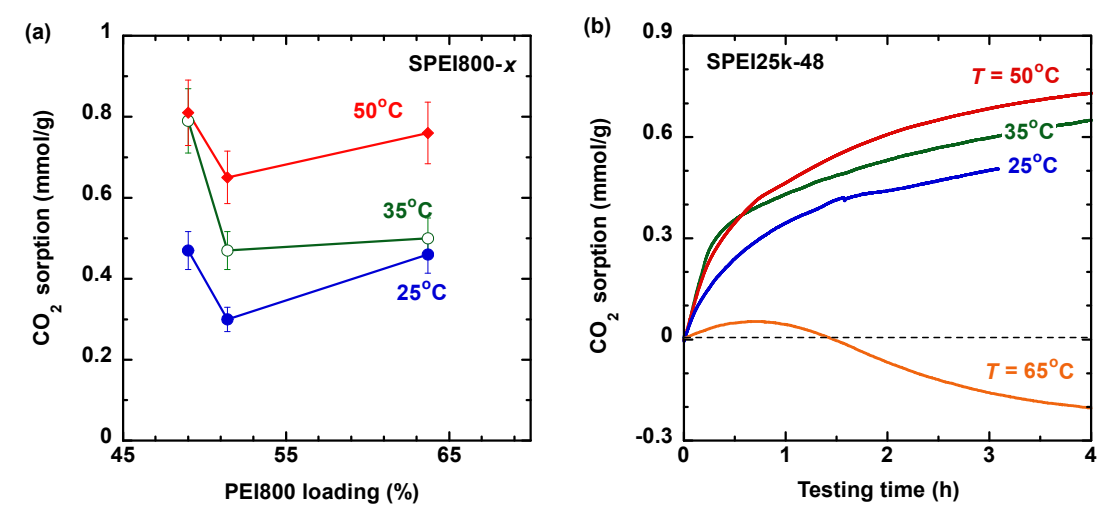


**Figure 4.** Effect of the PEI loading on (a) CO<sub>2</sub> sorption capacity and (b) amine efficiency when tested with 400 ppm CO<sub>2</sub> in air and 25 °C (dry gas). The error bars are estimated by the error propagation method.<sup>38</sup>

The amine efficiency for CO<sub>2</sub> sorption (mol CO<sub>2</sub>/mol N) can be calculated by assuming that only primary (1°) and secondary (2°) amines are active for CO<sub>2</sub> sorption under dry conditions (Equations 1 and 2). The branched PEI (including PEI800 and PEI25k) contains 1 mol N<sup>1°,2°</sup> per 62.3 g of PEI. As shown in Figure 4b, the amine efficiency of both SPEI25k and SPEI800 decreases from  $\approx$ 0.15 to  $\approx$ 0.07 mol CO<sub>2</sub>/mol N as *x* increases from 18% to 48%. The amine efficiency is significantly below the theoretical value of 0.5 mol CO<sub>2</sub>/mol N, indicating that not all amine groups are accessible for CO<sub>2</sub> sorption because of the CO<sub>2</sub> transport limit during the testing time (4 h). For example, the PEI800 is glassy at the testing temperature (25 °C) in SPEI800-35 ( $T_g = 38$  °C) and SPEI800-48 ( $T_g = 35$  °C), leading to low CO<sub>2</sub> diffusivity and limited access of CO<sub>2</sub> to the amine groups in the PEI films (Figure 3c).

Figure 5a exhibits that increasing the sorption temperature from 25 to 50 °C drastically increases the CO<sub>2</sub> sorption capacity of SPEI800 for 4-h testing. For example, increasing the temperature from 25 to 50 °C increases CO<sub>2</sub> sorption capacity by 72% from 0.47 to 0.81 mmol CO<sub>2</sub>/g in SPEI800-48, and by 36% from 0.53 to 0.72 mmol CO<sub>2</sub>/g for SPEI25k-48 (Figure 5b). The comparison indicates that the temperature effect is more significant for the lower

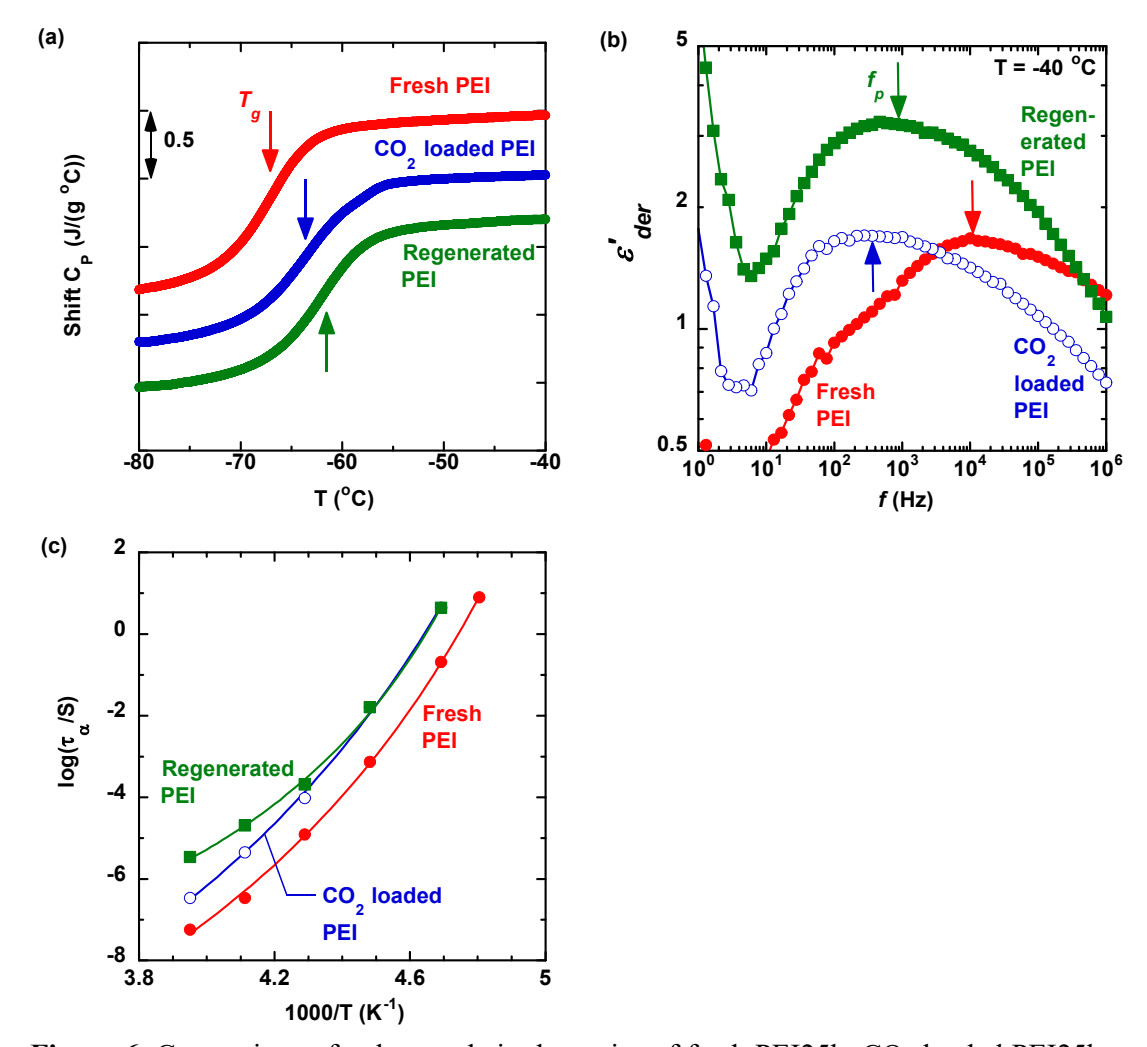
molecular weight PEI with lower viscosity. On the other hand, CO<sub>2</sub> sorption in SPEI25k-48 is below 0.1 mmol/g at 65 °C and eventually decreases to below zero after 4 h due to the degradation of PEI25k at 65 °C in the presence of O<sub>2</sub>.



**Figure 5.** (a) Effect of temperature on CO<sub>2</sub> sorption capacity in SPEI800 when tested with air containing 400 ppm CO<sub>2</sub>. (b) CO<sub>2</sub> sorption kinetics of SPEI25k-48 at 25, 35, 50, and 65 °C. The error bars in Figure 5a are estimated by the error propagation method.<sup>38</sup>

The increase in the measured CO<sub>2</sub> sorption with increasing temperature contradicts the notion that gas sorption at equilibrium decreases with increasing temperature. This behavior can be ascribed to the non-equilibrium CO<sub>2</sub> sorption caused by the restricted CO<sub>2</sub> diffusion in amines. As CO<sub>2</sub> reacts with the amine groups on the surface of the PEI films, it cross-links the PEI and lowers CO<sub>2</sub> diffusion in the PEI films to access other amine groups (Figure 3c). Increasing the temperature from 25 to 50 °C lowers the CO<sub>2</sub> content on the PEI surface and accelerates the CO<sub>2</sub> diffusion into the PEI films, resulting in higher CO<sub>2</sub> sorption. On the other hand, the effect of equilibrium solubility becomes dominant at 65 °C, decreasing the measured CO<sub>2</sub> sorption. The effect of diffusion-limited sorption is also evident when increasing the sorption time from 4 to 9 h increases CO<sub>2</sub> sorption capacity (Figure S2). Additionally, the SPEI25k-48 exhibits slower CO<sub>2</sub> sorption than SPEI800-48 because of the higher viscosity of PEI25k.

To validate the effect of the CO<sub>2</sub> sorption on the PEI chain dynamics, thermal properties were measured using DSC for three samples, including fresh PEI25k, PEI25k after CO<sub>2</sub> sorption, and regenerated PEI25k. The CO<sub>2</sub> sorption increases the  $T_g$  of the PEI, which agrees with neutron scattering experiments and computer simulations.<sup>35, 39</sup>



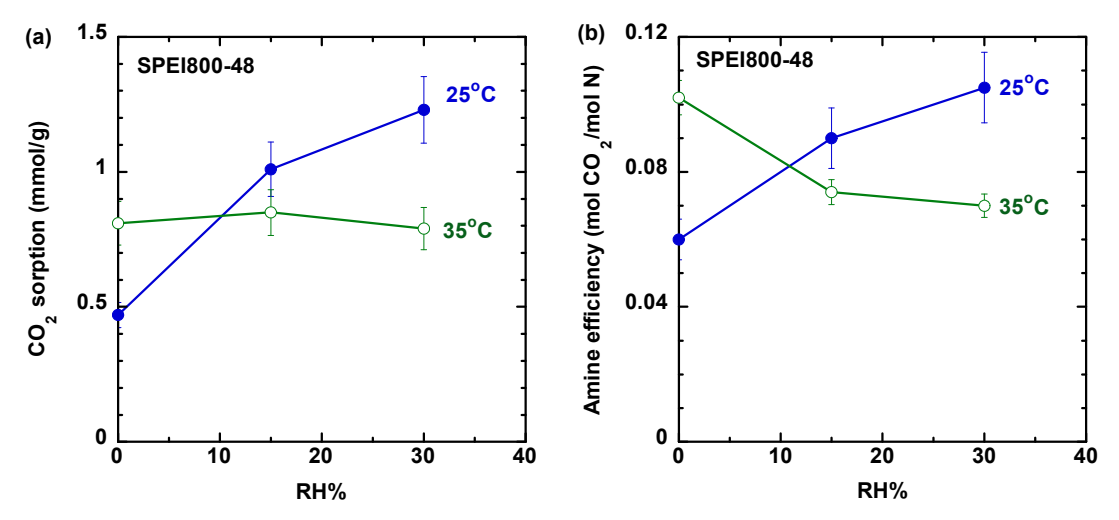
**Figure 6.** Comparison of polymer chain dynamics of fresh PEI25k, CO<sub>2</sub> loaded PEI25k, and regenerated PEI25k, including (a) DSC thermograms and (b) dielectric derivative spectra  $(\varepsilon'_{der})$  at -40 °C. The arrows point to the position of  $T_g$  in (a) and the peak frequency  $(f_p)$  associated with the segmental dynamics in (b). (c) Segmental relaxation estimated through  $\tau_{\alpha} = \frac{1}{2\pi f_p}$  at different temperatures. The lines provide the VFT fit to each sample.

Figure 6b shows a comparison of dielectric derivative spectra,  $\varepsilon'_{der} = -\frac{\pi}{2} \frac{\partial \varepsilon'}{\partial lnf}$  with  $\varepsilon'$  being the dielectric storage permittivity and f the frequency of fresh PEI, CO<sub>2</sub> loaded PEI, and

regenerated PEI. The arrows point to the characteristic segmental relaxation peaks of the PEI, and their structural relaxation can thus be estimated as  $\tau_{\alpha} = \frac{1}{2\pi f_p}$ . Both CO<sub>2</sub>-loaded and regenerated PEI exhibit much slower segmental relaxation with a significant broadening than the fresh PEI, implying the sorbent changes during sorbent regeneration. The results demonstrate that air-sorption and sorbent regeneration strongly affect the polyamine dynamics.

Figure 6c summarizes the temperature dependence of the  $\tau_{\alpha}$  for the three samples, where the symbols are from experiments, and the lines are the best fits of the Vogel-Fulcher-Tammann (VFT) equation. The  $T_g$  values from the VFT fit at  $\tau_{\alpha}=100\,s$  match well with those from the DSC measurements, which further confirms the peak assignment of our BDS measurements. We notice a shoulder peak at lower frequencies for all three samples. The physical origin of this peak remains unclear at this moment, which could be due to H-bonding association/dissociation in PEI among primary or secondary amine groups. The slow dynamics modes have also been observed in amine-based associative polymers through reversible H-bonding interactions.<sup>40</sup>

Effect of RH on CO<sub>2</sub> Sorption. Figure 7a illustrates the complicated effect of RH (15% and 30%) on the CO<sub>2</sub> sorption in SPEI800-48. The introduction of 15% RH increases the CO<sub>2</sub> sorption capacity at 25 °C from 0.47 to 1.0 mmol/g because of the additional reaction with the tertiary (3°) amine in the presence of water (Equations 3 and 4). Moreover, water swells the PEI network, permitting CO<sub>2</sub> access to additional amine sites. However, a further increase of the RH to 30% increases the CO<sub>2</sub> sorption capacity to only 1.2 mmol/g (12% improvement) at 25 °C, probably due to the competitive sorption between water and CO<sub>2</sub> with accessible amine groups and the swelling of the PEI and thus blocked pores in the SPEIs. 15



**Figure 7.** Effect of RH% on (a) CO<sub>2</sub> sorption capacity and (b) amine efficiency at 25 and 35 °C when tested with the air containing 400 ppm CO<sub>2</sub>. The error bars are estimated by the error propagation method.<sup>38</sup>

By contrast, the RH minimally affects the CO<sub>2</sub> sorption capacity at 35 °C, decreasing the amine efficiency presumably caused by the stronger binding between amine and H<sub>2</sub>O at 35 °C. The amine efficiency under humidified conditions was calculated assuming 1 mol N<sup>1°,2°,3°</sup> per 42.8 g of PEI instead of 1 mol N<sup>1°,2°</sup> per 62.3 g of PEI under dry condition. Figure 7b shows that the amine efficiency at 25 °C increases by  $\approx$ 72% from 0.061 to 0.10 mol CO<sub>2</sub>/mol N, suggesting that all amine types can sorb CO<sub>2</sub>. Interestingly, the amine efficiency at 35 °C is higher than that at 25 °C under dry conditions but 34% lower with 30% RH, signifying the complexity of CO<sub>2</sub> sorption behavior in the PEI-based membrane adsorbents.<sup>15</sup>

Regeneration Stability of Membrane Adsorbent. Sorbent regeneration ability is a key factor determining the DAC costs.<sup>41</sup> Regenerability is often characterized by the change in CO<sub>2</sub> sorption capacity during multiple sorption/desorption cycles. Figure 8a-b exhibits the sample mass as a function of time during the cycles for SPEI800-48 and SPEI25k-48, respectively, and their corresponding CO<sub>2</sub> sorption capacity for each cycle is summarized in Figure 8c. The SPEI25k-48 demonstrates a stable working capacity of 0.47 mmol/g after 3 cycles with minimal mass loss after desorption at 110 °C. By contrast, the CO<sub>2</sub> sorption

capacity of SPEI800-48 decreases by 29% from 0.66 to 0.47 mmol/g with a noticeable mass loss after each desorption step due to the evaporation and oxidative degradation of PEI800 by a trace amount of O<sub>2</sub>. After 5 cycles, SPEI800-48 exhibits a stable working capacity of 0.37 mmol/g.

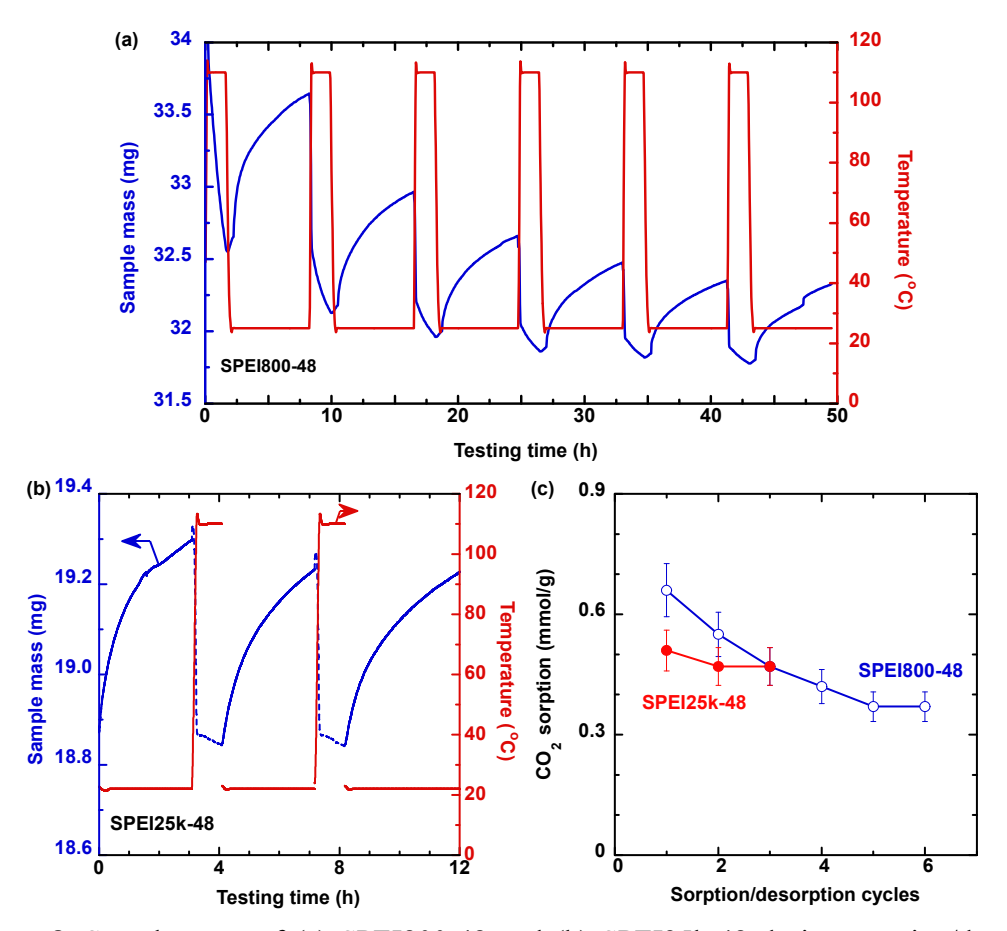


**Figure 8.** Sample mass of (a) SPEI800-48 and (b) SPEI25k-48 during sorption/desorption cycles, and (c) CO<sub>2</sub> sorption capacity for each cycle. The sorption was at 25 °C for 4 h with 400 ppm CO<sub>2</sub> in air, and the desorption was at 110 °C for 1 h under N<sub>2</sub> purge. The error bars in Figure 8c are estimated by the error propagation method.<sup>38</sup>

SPEI800-48 was evaluated for 18 cycles of accelerated sorption and desorption to determine its regenerability (Figure S3). The sorption was conducted at 25 °C with 400 ppm CO₂ in air for 2 h, and the desorption was performed at 110 °C under N₂ for 15 min. SPEI800-48 exhibits a stable working capacity of ≈0.10 mmol/g after 10 cycles, indicating a slow sorption kinetic of this membrane adsorbent.

#### **■ CONCLUSION**

We develop low-cost and scalable membrane adsorbents for DAC of CO<sub>2</sub> based on a commercially available, thermally stable flatsheet polymeric substrate (Solupor). Branched PEIs with molecular masses of 800 and 25k g/mol were successfully impregnated into the pores, and the loading is determined by weight and TGA and agrees well with the PEI concentration in the solutions and the measured porosity. Interestingly, the impregnated PEI forms thin films on the pore walls and exhibits much higher  $T_g$  and better thermal stability than the bulk PEI. CO<sub>2</sub> sorption by these membrane adsorbents is limited by its diffusion, and increasing the PEI loading increases CO2 sorption capacity but decreases amine efficiency because of the thicker PEI layers. Increasing the temperature from 25 to 50 °C enhances the CO<sub>2</sub> sorption capacity by 72% in SPEI800-48 because of the enhanced diffusivity at 50 °C. SPEI800-48 exhibits the highest sorption capacity of 1.2 mmol/g at 25 °C and 30% RH with the air containing 400 ppm CO<sub>2</sub>, and such a sorption capacity is comparable with state-of-theart commercial sorbents. SPEI25k-48 exhibits a stable working capacity of 0.47 mmol/g after 3 cycles, while SPEI800-48 exhibits a working capacity of 0.37 mmol/g. This work demonstrates the potential of low-cost polymeric substrates to prepare PEI-based adsorbent with low resistance to airflow and comparable CO<sub>2</sub> sorption capacity.

### **■ EXPERIMENTAL SECTION**

**Materials.** Branched PEI800, branched PEI25k, and n-decane were obtained from Sigma Aldrich (St. Louis, MO). Methanol was purchased from Fisher Scientific International (Pittsburgh, PA). Cylinders of N<sub>2</sub>, zero-grade air, and air containing 1200 ppm CO<sub>2</sub> were obtained from Airgas (Radnor, PA).

**Preparation of Membrane Adsorbents.** Membrane adsorbents with different loadings of PEI in Solupor were prepared using a wet impregnation method.<sup>30</sup> First, a desired amount of PEI was dissolved in methanol, which can then easily wet the hydrophobic Solupor support. Second, a Solupor sample with an initial mass of  $m_0$  (mg) was immersed in the solution overnight. Third, the impregnated support was removed from the solution, dried in the air, and dried under a vacuum overnight at 22 °C. The impregnated support was measured to have a mass of  $m_1$  (mg). Different PEI loadings were obtained by varying the PEI concentration in the methanol solutions. The PEI loading, x (mass%), was calculated using in Equation 8:

$$x = \frac{m_1 - m_0}{m_1} \times 100\% \tag{8}$$

**Physical Properties Characterization.** Thermal stability and PEI content in the sorbents were determined by TGA (TG 209 F1, Netzsch GmbH & Co., Germany) under the N<sub>2</sub> atmosphere. The samples were first equilibrated at 100 °C for 1 h and then heated to 800 °C at 10 °C/min. The  $T_g$  of the samples was determined using DSC (Q2000, TA Instruments, New Castle, DE). The samples were first equilibrated at -90 °C for 10 mins and then heated to 80 °C at 10 °C/min, and the second heating thermogram was used to derive T<sub>g</sub>.

BDS was employed to characterize the influence of  $CO_2$  sorption and sorbent regeneration on the dynamics of PEI. Three samples were measured for comparison, including the fresh PEI, the CO<sub>2</sub>-loaded PEI, and the regenerated PEI after CO<sub>2</sub> sorption and desorption. Specifically, a thin film of PEI was filled in a hollow Teflon spacer with an outer diameter of 25 mm and an inner diameter of 14 mm. The PEI-filled Teflon spacer was then sandwiched by two gold electrodes with a diameter of 20 mm and transferred into a ZGS sample holder connected to Novocontrol Concept 40. The ZGS sample holder was then placed in an environmental chamber with a temperature accuracy of  $\pm 0.1$  °C controlled by a Quatro System. Each measurement covers a frequency range of  $10^7 - 10^{-2}$  HZ and a temperature range from - 100 to 40 °C upon heating at an interval of 5 °C and from 40 to -100 °C upon cooling at an

interval of 20 °C. The spectra of the heating and cooling processes were compared to confirm the reproducibility of the measurements. Before each measurement, a thermal annealing of 20 mins was applied to ensure thermal equilibrium.

The membrane morphology was characterized by FIB-SEM (Auriga CrossBeam, Carl Zeiss, Germany). BET surface area was determined using N<sub>2</sub> adsorption isotherm (Tri-Star II, Micromeritics, Norcross, GA). The sorbent porosity,  $\phi_{MA}$  (%), was determined by n-decane uptake using the following equation:

$$\phi_{MA} = \frac{m_2 - m_1}{\rho_L} \frac{1}{V_{MA}} \tag{9}$$

where  $m_1$  and  $m_2$  are the sample mass before and after the n-decane uptake.  $\rho_L$  (g/cm<sup>3</sup>) is the density of n-decane (0.73 g/cm<sup>3</sup>), and  $V_{MA}$  (cm<sup>3</sup>) is the volume of the sorbent sample. Pure-gas CO<sub>2</sub> permeance was determined using a constant-pressure and variable-volume apparatus at 15 psig and 35 °C.<sup>37</sup>

Characterization of DAC Performance by TGA. The CO<sub>2</sub> sorption capacity of the membrane adsorbents was determined using TGA. First, a sample of 30 – 45 mg was heated to 110 °C at 10 °C/min under an N<sub>2</sub> environment (90 cm<sup>3</sup>/min) and then kept for 1 h to remove H<sub>2</sub>O and CO<sub>2</sub>. The flow rate is sufficiently high to minimize concentration polarization on the sample surface. Second, the sample was cooled to the desired sorption temperatures of 25, 35, or 50 °C and then kept at the temperature for 20 min. Third, the gas was switched to the simulated air containing 400 ppm CO<sub>2</sub> while retaining the gas flow rate at 90 cm<sup>3</sup>/min. Finally, after 4-h sorption, the sample was heated to 110 °C under N<sub>2</sub> for CO<sub>2</sub> desorption.

To investigate the effect of humidity on CO<sub>2</sub> sorption capacity, the sample was first allowed to saturate with water vapor for 2 h at the desired RH% under N<sub>2</sub> atmosphere. Then 400 ppm CO<sub>2</sub> was introduced to TGA at the same RH% by passing a gas stream through a temperature-controlled gas bubbler. The stability and regenerability of the adsorbent were also evaluated by multiple cycles of sorption/desorption.

### ■ ASSOCIATED CONTENT

## **Supporting Information**

The Supporting Information is available free of charge at https://pubs.acs.org.

TGA thermograms; physical properties; CO<sub>2</sub> sorption with time

# ■ AUTHOR INFORMATION

## **Corresponding Author**

**Haiqing Lin** – Department of Chemical and Biological Engineering, University at Buffalo, The State University of New York, Buffalo, NY 14260, USA; orcid.org/0000-0001-8042-154X; Email: haiqingl@buffalo.edu

## Authors

**Thien Tran** – Department of Chemical and Biological Engineering, University at Buffalo, The State University of New York, Buffalo, NY 14260, USA; orcid.org/0000-0002-3517-8322

Shweta Singh – Department of Chemical and Biological Engineering, University at Buffalo, The State University of New York, Buffalo, NY 14260, USA

Shiwang Cheng – Department of Chemical Engineering and Materials Science, Michigan State University, East Lansing, MI 48824, USA; orcid.org/0000-0001-7396-4407

## **Author Contributions**

All authors contributed to the scientific discussion and manuscript preparation. H.L. and T.T. conceived the approach and conducted experimental designs. T.T. and S.S. fabricated and characterized materials. T.T. wrote the first draft of the manuscript, and all authors contributed to manuscript editing. H.L. supervised the project.

## **Notes**

The authors declare no competing financial interest.

## ■ ACKNOWLEDGMENT

This work received financial support from the U.S. Department of Energy National Energy Technology Laboratory (DE-FE0031960) and the National Science Foundation (NSF # 2230728).

# **■ REFERENCES**

- (1) Keith, D. W.; Holmes, G.; Angelo, D. S.; Heidel, K., A Process for Capturing CO<sub>2</sub> from the Atmosphere, *Joule* **2018**, *2* (8), 1573-1594.
- (2) Erans, M.; Sanz-Perez, E. S.; Hanak, D. P.; Clulow, Z.; Reiner, D. M.; Mutch, G. A., Direct Air Capture: Process Technology, Techno-Economic and Socio-Political Challenges, *Energy Environ. Sci.* **2022**, *15* (4), 1360-1405.
- (3) House, K. Z.; Baclig, A. C.; Ranjan, M.; van Nierop, E. A.; Wilcox, J.; Herzog, H. J., Economic and Energetic Analysis of Capturing CO<sub>2</sub> from Ambient Air, *PNAS* **2011**, *108* (51), 20428-20433.
- (4) Azarabadi, H.; Lackner, K. S., Postcombustion Capture or Direct Air Capture in Decarbonizing US Natural Gas Power?, *Environ. Sci. Techn.* **2020**, *54* (8), 5102-5111.
- (5) Azarabadi, H.; Lackner, K. S., A Sorbent-Focused Techno-Economic Analysis of Direct Air Capture, *Appl. Energy* **2019**, *250*, 959-975.
- (6) Shi, X.; Xiao, H.; Azarabadi, H.; Song, J.; Wu, X.; Chen, X.; Lackner, K. S., Sorbents for the Direct Capture of CO<sub>2</sub> from Ambient Air, *Angew. Chem. Int. Ed.* **2020**, *59* (18), 6984-7006.
- (7) Sanz-Perez, E. S.; Murdock, C. R.; Didas, S. A.; Jones, C. W., Direct Capture of CO<sub>2</sub> from Ambient Air, *Chem. Rev.* **2016**, *116* (19), 11840-11876.
- (8) Lee, W. H.; Zhang, X.; Banerjee, S.; Jones, C. W.; Realff, M. J.; Lively, R. P., Sorbent-Coated Carbon Fibers for Direct Air Capture Using Electrically Driven Temperature Swing Adsorption, *Joule* **2023**, *7* (6), 1241-1259.
- (9) Hosseini, A. A.; Lashaki, M. J., A Comprehensive Evaluation of Amine-Impregnated Silica Materials for Direct Air Capture of Carbon Dioxide, *Sep. Purif. Techn.* **2023**, 325.
- (10) Hack, J.; Maeda, N.; Meier, D. M., Review on CO<sub>2</sub> Capture Using Amine-Functionalized Materials, *ACS Omega* **2022**, *7* (44), 39520-39530.
- (11) Tong, Z.; Ho, W. S. W., New Sterically Hindered Polyvinylamine Membranes for CO<sub>2</sub> Separation and Capture, *J. Membr. Sci.* **2017**, *543*, 202-211.
- (12) Varghese, A. M.; Karanikolos, G. N., CO<sub>2</sub> Capture Adsorbents Functionalized by Amine–bearing Polymers: A Review, *Int. J. Greenh. Gas Con.* **2020**, *96*, 103005.
- (13) Wang, X.; Fujii, M.; Wang, X.; Song, C., New Approach to Enhance CO<sub>2</sub> Capture of "Molecular Basket" Sorbent by Using 3-AminopropyltriethOxysilane to Reshape Fumed Silica Support, *Ind. Eng. Chem. Res.* **2020**, *59* (15), 7267-7273.

- (14) Guo, X.; Ding, L.; Kanamori, K.; Nakanishi, K.; Yang, H., Functionalization of Hierarchically Porous Silica Monoliths with Polyethyleneimine (PEI) for CO<sub>2</sub> Adsorption, *Micropor. Mesopor. Mat.* **2017**, *245*, 51-57.
- (15) Chen, J.; Moon, H.; Kim, K.; Choi, J.; Narayanan, P.; Sakwa-Novak, M. A.; Jones, C. W.; Jang, S., Distribution and Transport of CO<sub>2</sub> in Hyperbranched Poly(ethylenimine)-Loaded MCM-41: A Molecular Dynamics Simulation Approach, ACS Appl. Mater. Interfaces 2023, 15 (37), 43678-43690.
- (16) Miao, Y.; Wang, Y.; Ge, B.; He, Z.; Zhu, X.; Li, J.; Liu, S.; Yu, L., Mixed Diethanolamine and Polyethyleneimine with Enhanced CO<sub>2</sub> Capture Capacity from Air, *Adv. Sci.* **2023**, *10* (16), 2207253.
- (17) Gelles, T.; Rezaei, F., Diffusion Kinetics of CO<sub>2</sub> in Amine-Impregnated MIL-101, Alumina, and Silica Adsorbents, *AIChE J.* **2020**, *66* (1), e16785.
- (18) He, Y.; Boone, P.; Lieber, A. R.; Tong, Z.; Das, P.; Hornbostel, K. M.; Wilmer, C. E.; Rosi, N. L., Implementation of a Core-Shell Design Approach for Constructing MOFs for CO<sub>2</sub> Capture, *ACS Appl. Mater. Interfaces* **2023**, *15* (19), 23337-23342.
- (19) McDonald, T. M.; Mason, J. A.; Kong, X.; Bloch, E. D.; Gygi, D.; Dani, A.; Crocella, V.; Giordanino, F.; Odoh, S. O.; Drisdell, W. S.; Vlaisavljevich, B.; Dzubak, A. L.; Poloni, R.; Schnell, S. K.; Planas, N.; Lee, K.; Pascal, T.; Wan, L. W. F.; Prendergast, D.; Neaton, J. B.; Smit, B.; Kortright, J. B.; Gagliardi, L.; Bordiga, S.; Reimer, J. A.; Long, J. R., Cooperative Insertion of CO<sub>2</sub> in Diamine-Appended Metal-Organic Frameworks, *Nature* 2015, 519 (7543), 303-308.
- (20) Shin, S.; Yoo, D. K.; Bae, Y. S.; Jhung, S. H., Polyvinylamine-Loaded Metal-Organic Framework MIL-101 for Effective and Selective CO<sub>2</sub> Adsorption Under Atmospheric or Lower Pressure, *Chem. Eng. J.* **2020**, *389*, 123429.
- (21) Rim, G.; Priyadarshini, P.; Song, M.; Wang, Y.; Bai, A.; Realff, M. J.; Lively, R. P.; Jones, C. W., Support Pore Structure and Composition Strongly Influence the Direct Air Capture of CO<sub>2</sub> on Supported Amines, *J. Am. Chem. Soc.* **2023**, *145* (13), 7190-7204.
- (22) Short, G. N.; Burentugs, E.; Proano, L.; Moon, H. J.; Rim, G.; Nezam, I.; Korde, A.; Nair, S.; Jones, C. W., Single-Walled Zeolitic Nanotubes: Advantaged Supports for Poly(ethylenimine) in CO<sub>2</sub> Separation from Simulated Air and Flue Gas, *JACS Au* **2023**, *3* (1), 62-69.
- (23) Zhu, L.; Tian, D.; Shin, D.; Jia, W.; Bae, C.; Lin, H., Effects of Tertiary Amines and Quaternary Ammonium Halides in Polysulfone on Membrane Gas Separation Properties, J. Polym. Sci. Part B: Polym. Phys. 2018, 56 (18), 1239-1250.
- (24) Kumar, P.; Kim, S.; Ida, J.; Guliants, V. V., Polyethyleneimine-Modified MCM-48 Membranes: Effect of Water Vapor and Feed Concentration on N<sub>2</sub>/CO<sub>2</sub> Selectivity, *Ind. Eng. Chem. Res.* **2008**, *47* (1), 201-208.
- (25) Ma, X.; Wang, X.; Song, C., "Molecular Basket" Sorbents for Separation of CO<sub>2</sub> and H<sub>2</sub>S from Various Gas Streams, *J. Am. Chem. Soc.* **2009**, *131*, 5777-5783.
- (26) Min, Y. J.; Ganesan, A.; Realff, M. J.; Jones, C. W., Direct Air Capture of CO<sub>2</sub> Using Poly(ethyleneimine)-Functionalized Expanded Poly(tetrafluoroethylene)/Silica Composite Structured Sorbents, ACS Appl. Mater. Interfaces 2022, 14 (36), 40992-41002.
- (27) Lively, R. P.; Chance, R. R.; Kelley, B. T.; Deckman, H. W.; Drese, J. H.; Jones, C. W.; Koros, W. J., Hollow Fiber Adsorbents for CO<sub>2</sub> Removal from Flue Gas, *Ind. Eng. Chem. Res.* 2009, 48 (15), 7314-7324.
- (28) Armstrong, M.; Shi, X.; Shan, B.; Lackner, K.; Mu, B., Rapid CO<sub>2</sub> Capture from Ambient Air by Sorbent-Containing Porous Electrospun Fibers Made with the Solvothermal Polymer Additive Removal Technique, *AIChE J.* **2019**, *65* (1), 214-220.

- (29) Kong, F.; Rim, G.; Priyadarshini, P.; Song, M.; Realff, M. J. J.; Lively, R. P. P.; Jones, C. W. W., Dynamic Study of Direct CO<sub>2</sub> Capture from Indoor Air Using Poly(ethylenimine)-Impregnated Fiber Sorbents, *Sustain.* **2023**, *7* (18), 4461-4473.
- (30) Zhao, S.; Huang, K.; Lin, H., Impregnated Membranes for Water Purification Using Forward Osmosis, *Ind. Eng. Chem. Res.* **2015**, *54* (49), 12354-12366.
- (31) Li, K.; Jiang, J.; Yan, F.; Tian, S.; Chen, X., The Influence of Polyethyleneimine Type and Molecular Weight on the CO<sub>2</sub> Capture Performance of PEI-Nano Silica Adsorbents, *Appl. Energy* **2014**, *136*, 750-755.
- (32) Goeppert, A.; Meth, S.; Prakash, G. S.; Olah, G. A., Nanostructured Silica as A Support for Regenerable High-Capacity Organoamine-Based CO<sub>2</sub> Sorbents, *Energy Environ. Sci.* **2010**, *3* (12), 1949-1960.
- (33) Singh, R. K.; Ruj, B.; Sadhukhan, A. K.; Gupta, P., Thermal Degradation of Waste Plastics Under Non-Sweeping Atmosphere: Part 1: Effect of Temperature, Product Optimization, and Degradation Mechanism, *J. Environ. Manage.* **2019**, *239*, 395-406.
- (34) Choi, S.; Gray, M. L.; Jones, C. W., Amine-Tethered Solid Adsorbents Coupling High Adsorption Capacity and Regenerability for CO<sub>2</sub> Capture From Ambient Air, *ChemSusChem* **2011**, *4* (5), 628-635.
- (35) Carrillo, J.-M. Y.; Sakwa-Novak, M. A.; Holewinski, A.; Potter, M. E.; Rother, G.; Jones, C. W.; Sumpter, B. G., Unraveling the Dynamics of Aminopolymer/Silica Composites, *Langmuir* **2016**, *32* (11), 2617-2625.
- (36) Yavari, M.; Maruf, S.; Ding, Y.; Lin, H., Physical Aging of Glassy Perfluoropolymers in Thin Film Composite Membranes. Part II. Glass Transition Temperature and The Free Volume Model, *J. Membr. Sci.* **2017**, *525*, 399-408.
- (37) Zhang, G.; Bui, V. T.; Yin, Y.; Tsai, E. H. R.; Nam, C.-Y.; Lin, H., Carbon Capture Membranes Based on Amorphous Polyether Nanofilms Enabled by Thickness Confinement and Interfacial Engineering, *ACS Appl. Mater. Interfaces* **2023**, *15* (29), 35543-35551.
- (38) Bevington, P. R.; Robinson, D. K., *Data Reduction and Error Analysis for the Physical Sciences*. 2nd ed.; McGraw-Hill, Inc.: New York, 1992.
- (39) Holewinski, A.; Sakwa-Novak, M. A.; Carrillo, J.-M. Y.; Potter, M. E.; Ellebracht, N.; Rother, G.; Sumpter, B. G.; Jones, C. W., Aminopolymer Mobility and Support Interactions in Silica-PEI Composites for CO<sub>2</sub> Capture Applications: A Quasielastic Neutron Scattering Study, *J. Phys. Chem. B* **2017**, *121* (27), 6721-6731.
- (40) Xing, K.; Tress, M.; Cao, P.; Cheng, S.; Saito, T.; Novikov, V. N.; Sokolov, A. P., Hydrogen-Bond Strength Changes Network Dynamics in Associating Telechelic PDMS, *Soft Matter* **2018**, *14* (7), 1235-1246.
- (41) Carneiro, J. S. A.; Innocenti, G.; Moon, H. J.; Guta, Y.; Proano, L.; Sievers, C.; Sakwa-Novak, M. A.; Ping, E. W.; Jones, C. W., Insights into the Oxidative Degradation Mechanism of Solid Amine Sorbents for CO<sub>2</sub> Capture from Air: Roles of Atmospheric Water, *Angew. Chem. Int. Ed.* **2023**, *62* (24), e202302887.

# **Graphic Abstract**

Scalable and Highly Porous Membrane Adsorbents for Direct Air Capture of CO<sub>2</sub>

